

Selective metastatic tumor labeling with green fluorescent protein and killing by systemic administration of telomerase-dependent adenoviruses

Hiroyuki Kishimoto,^{1,2,3} Yasuo Urata,⁵
Noriaki Tanaka,³ Toshiyoshi Fujiwara,^{3,4}
and Robert M. Hoffman^{1,2}

¹AntiCancer, Inc.; ²Department of Surgery, University of California, San Diego, California; ³Division of Surgical Oncology, Department of Surgery, Okayama University Graduate School of Medicine, Dentistry and Pharmaceutical Sciences; ⁴Center for Gene and Cell Therapy, Okayama University Hospital, Okayama, Japan; and ⁵Oncolys BioPharma, Inc., Tokyo, Japan

Abstract

We previously constructed telomerase-dependent, replication-selective adenoviruses OBP-301 (Telomelysin) and OBP-401 [Telomelysin-green fluorescent protein (GFP); TelomeScan], the replication of which is regulated by the human telomerase reverse transcriptase promoter. By intratumoral injection, these viruses could replicate within the primary tumor and subsequent lymph node metastasis. The aim of the present study was to evaluate the possibility of systemic administration of these telomerase-dependent adenoviruses. We assessed the antitumor efficacy of OBP-301 and the ability of OBP-401 to deliver GFP in hepatocellular carcinoma (HCC) and metastatic colon cancer nude mouse models. We showed that i.v. administration of OBP-301 significantly inhibited colon cancer liver metastases and orthotopically implanted HCC. Further, we showed that OBP-401 could visualize liver metastases by tumor-specific expression of the *GFP* gene after portal venous or i.v. administration. Thus, systemic administration of these adenoviral vectors should have clinical potential to treat and detect liver metastasis and HCC. [Mol Cancer Ther 2009;8(11):3001–8]

Introduction

Primary and metastatic liver tumors are a common cause of death throughout the world. Hepatocellular carcinoma

(HCC), the most common primary liver tumor, is the fifth most common malignancy and the third most frequent cause of cancer death worldwide (1, 2). HCC often metastasizes widely, and distant metastatic sites include lung, bone, adrenals, and brain. The 5-year survival rates of these patients are usually in the range of 16% to 25% (3). Colorectal cancer is also one of the most common tumors worldwide. The liver is the most preferential site for metastasis of colorectal cancer and over half of these patients die from their metastatic liver diseases (4). Therefore, management of the liver metastases is a key factor for colorectal cancer prognosis.

Liver resection is the only potentially curative treatment option available for patients with primary and metastatic liver tumors (5, 6). However, because only a minority of patients with colorectal liver metastases or HCC are candidates for surgery (7–10), new therapeutic agents and innovative approaches for tumor detection are desired.

We previously constructed two conditionally replicating type 5 adenoviruses OBP-301 (Telomelysin) and OBP-401 [Telomelysin-green fluorescent protein (GFP); TelomeScan]. The replication of these viruses is regulated by the human telomerase reverse transcriptase (hTERT) promoter (11–15). hTERT is the catalytic subunit of telomerase, which is highly active in cancer cells but quiescent in most normal somatic cells (16). Therefore, these adenoviruses have tumor-specific replication regulated by the hTERT transcriptional activity. OBP-301 has shown a strong anticancer efficacy in a variety of tumors *in vitro* and *in vivo* (11, 12, 17–19). We also reported that OBP-401 can replicate in and label cancer cells with GFP *in vitro* and *in vivo* and thereby enables imaging of tumor cells by GFP fluorescence *in vivo* (15). Tumor specificity is conferred by selective replication of OBP-401 in the cancer cells. Replication of the virus, and therefore production of GFP, depends on the tumor-specific expression of telomerase. In those studies, however, the virus was administered locally such as by intratumoral injection or administration into a body cavity (thoracic or abdominal cavity). The efficacy of these viruses, when administered systemically, has not been evaluated.

In the present study, we examined the feasibility of systemic administration of OBP-301 and OBP-401 to colorectal liver metastases and to orthotopic HCC tumor in nude mice models, focusing on the antitumor efficacy of OBP-301 and the ability of OBP-401 to selectively induce *GFP* gene expression in cancer cells.

Materials and Methods

Recombinant Adenovirus

We previously constructed OBP-301, in which the hTERT promoter element drives the expression of the *E1A* and *E1B* genes linked with an internal ribosome entry site (11–14).

Received 6/22/09; revised 8/17/09; accepted 9/1/09; published OnlineFirst 11/3/09.

Grant support: National Cancer Institute grant CA132242.

The costs of publication of this article were defrayed in part by the payment of page charges. This article must therefore be hereby marked *advertisement* in accordance with 18 U.S.C. Section 1734 solely to indicate this fact.

Requests for reprints: Robert M. Hoffman, AntiCancer, Inc., San Diego, CA 92111. Phone: 858-654-2555, Fax: 858-268-4175. E-mail: all@anticancer.com

Copyright © 2009 American Association for Cancer Research.

doi:10.1158/1535-7163.MCT-09-0556

OBP-401, was derived from OBP-301 and also contains the GFP gene under the control of the cytomegalovirus promoter, was also constructed previously (15, 20). These viruses were purified by ultracentrifugation in cesium chloride step gradients. Their titers were determined by a plaque-forming assay using 293 cells. The viruses were stored at -80°C .

Cell Culture

The human colorectal cancer cell line HCT-116 and the human HCC cell lines Hep3B and HepG2 were obtained from the American Type Culture Collection. The cells were cultured in RPMI 1640 (Irvine Scientific) supplemented with 10% fetal bovine serum.

GFP Gene Transduction of Cancer Cells

For GFP gene transduction of cancer cells, 20% confluent HCT-116 or Hep3B cells were incubated with a 1:1 precipitated mixture of retroviral supernatants of the PT67 GFP-expressing packaging cells and RPMI 1640 containing 10% fetal bovine serum for 72 h. Fresh medium was replenished at this time. Tumor cells were harvested by trypsin/EDTA 72 h post-transduction and subcultured at a ratio of 1:15 in-

to selective medium containing 200 $\mu\text{g}/\text{mL}$ G418. The level of G418 was increased up to 800 $\mu\text{g}/\text{mL}$ in a stepwise manner. GFP-expressing cancer cells were isolated with cloning cylinders (Bel-Art Products) using trypsin/EDTA and amplified by conventional culture methods in the absence of selective agent.

Animal Experiments

Athymic nude mice were kept in a barrier facility under HEPA filtration and fed with autoclaved laboratory rodent diet (Teklad LM-485; Western Research Products). All animal studies were conducted in accordance with the principles and procedures outlined in the NIH Guide for the Care and Use of Laboratory Animals under assurance no. A3873-1. All animal procedures were done under anesthesia using s.c. administration of a ketamine mixture (10 μL ketamine HCl, 7.6 μL xylazine, 2.4 μL acepromazine maleate, and 10 μL PBS).

Experimental Liver Metastasis Model of Human Colon Cancer

To generate a liver metastasis model, unlabeled HCT-116 or HCT-116-GFP human colon cancer cells were injected

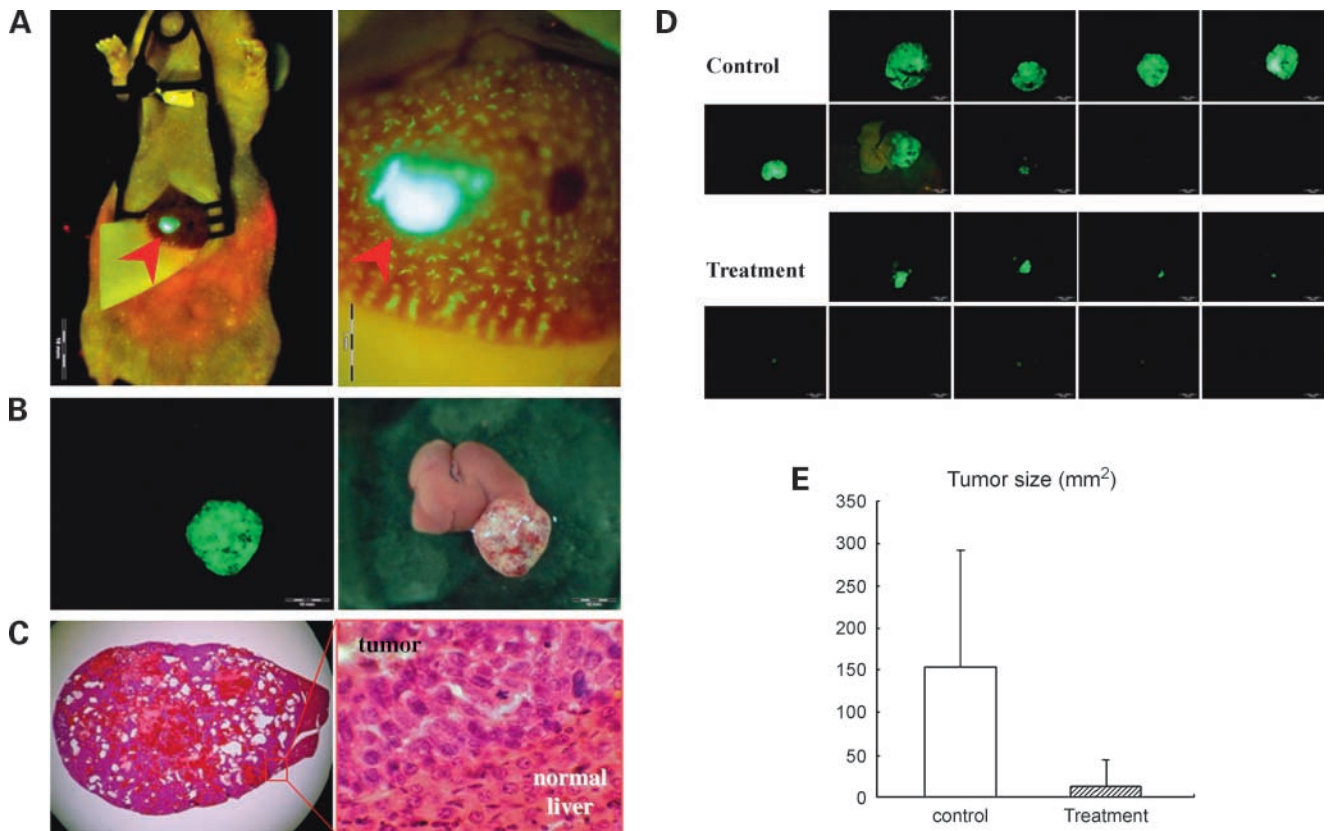


Figure 1. Efficacy of systemic OBP-301 administration on orthotopic HCC. **A**, Hep3B-GFP cells were subserosally injected into the left lobe of the liver (red arrow) to generate an orthotopic liver tumor model (left). Some cells could be seen accumulating in the terminal portal veins near the bleb of the injected site (right). **B**, macroscopic appearance of Hep3B-GFP liver tumor 8 wk after inoculation. Left, fluorescence detection; right, bright-field observation. **C**, H&E staining of Hep3B-GFP liver tumor section. Left, magnification, $\times 10$; right, detail of the boxed region. Magnification, $\times 400$. **D**, macroscopic appearance of liver. Livers were excised 8 wk after Hep3B-GFP cells injection. OBP-301 or PBS were i.v. injected biweekly starting from 2 wk after tumor cell inoculation. Excised livers were photographed under fluorescence. **E**, quantitative analysis of the tumor size (fluorescent area) of control and OBP-301-treated mice ($P < 0.01$).

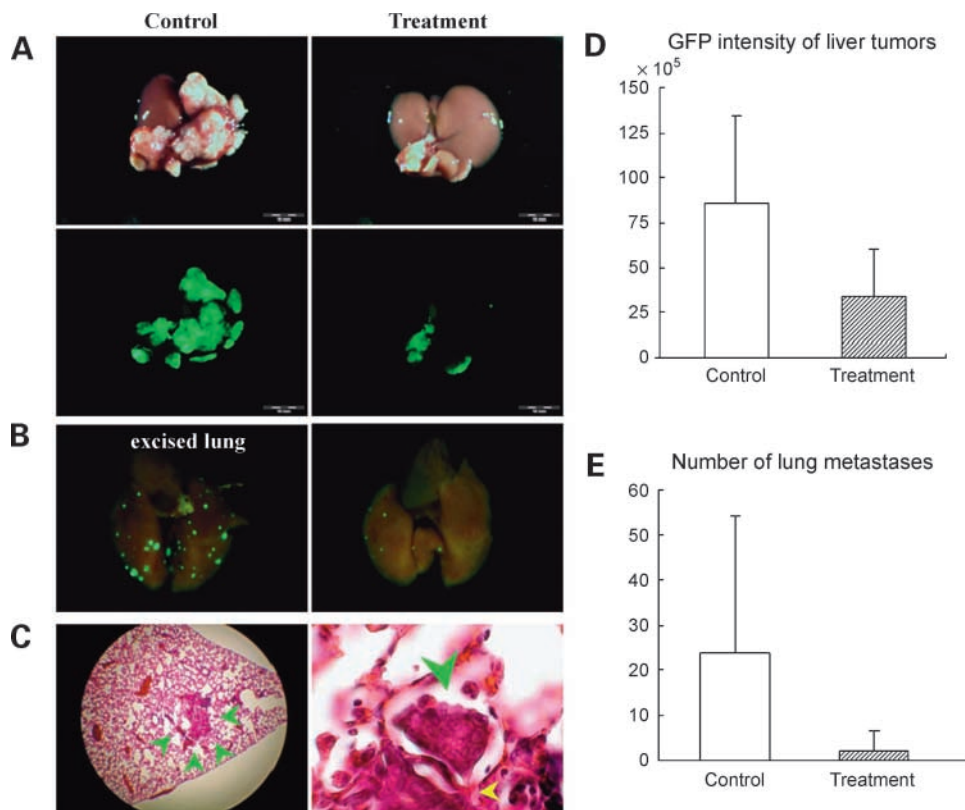


Figure 2. Systemic OBP-301 therapy of colon cancer liver metastases. **A**, macroscopic appearance of livers. HCT-116-GFP cells were injected into the spleen of nude mice, and the liver was excised 6 wk later. OBP-301 or PBS were i.v. injected 5 d after tumor cell inoculation. Excised livers were photographed under bright light (*top*). Fluorescence imaging showed GFP expression signals on the HCT-116-GFP liver metastasis (*bottom*). **B**, macroscopic appearance of lungs. Lung metastatic foci were detected with GFP fluorescence. *Left*, control; *right*, OBP-301 treatment significantly suppressed lung metastasis. **C**, H&E staining of lung metastasis in control mouse (*green arrow*). *Left*, magnification, $\times 40$; *right*, protrusion of tumor (*green arrow*) into the adjacent alveoli through the Kohn's pore (*yellow arrow*). Magnification, $\times 400$. **D**, quantitative analysis of the total GFP intensity in the liver of control and OBP-301-treated mice ($P < 0.05$). **E**, quantitative analysis of the number of lung metastases of control and OBP-301-treated mice ($P < 0.05$).

at a density of 2×10^6 in 50 μ L Matrigel (BD Biosciences) into the spleen of nude mice through a 28-gauge needle at laparotomy.

Orthotopic Liver Tumor Model of HCC

An orthotopic liver tumor model with human HCC was made with unlabeled Hep3B or Hep3B-GFP human HCC cells. Unlabeled Hep3B or Hep3B-GFP cells (5.0×10^6 in 10 μ L Matrigel) were subserosally injected into the left lobe of the liver through a 28-gauge needle at laparotomy. Unlabeled HepG2 cells, cells (3×10^6 in 50 μ L Matrigel) were injected into the spleen of nude mice through a 28-gauge needle at laparotomy.

Antitumor Efficacy Studies

To assess the antitumor efficacy of i.v. administration of OBP-301 against liver metastases of the colorectal cancer, OBP-301 was injected once systemically into the tail vein at a dose of 5×10^8 plaque forming units (PFU)/100 μ L 5 days after HCT-116-GFP cells were injected into the spleen. Control mice were injected with 100 μ L PBS in an identical manner ($n = 9$ mice per group). Six weeks after tumor cell inoculation (5 weeks after treatment), fluorescence imaging was done using an Olympus OV100 Imaging System. GFP

fluorescent intensity of the liver metastases and the number of lung metastases were determined. To obtain GFP intensity, exposure conditions were maintained constant at 30 ms to keep the data comparable. GFP intensity was quantified and presented in the units of SUM green intensity using Cell software (Olympus-Biosystems). The experimental data are presented as mean \pm SD. Comparison of the GFP intensity and the number of lung metastases between the treatment and control groups were analyzed using a two-tailed Student's *t* test.

The antitumor efficacy of i.v. administration of OBP-301 was also assessed in an orthotopic liver tumor model of HCC. OBP-301 was i.v. injected biweekly (5×10^8 PFU/2 weeks for 6 weeks) starting from 2 weeks after Hep3B-GFP cells were injected into the liver. Control mice were injected with 100 μ L PBS in an identical manner ($n = 9$ mice per group). All animals were examined 8 weeks after cancer cell inoculation (2 weeks after last treatment). Development of tumor growth and response to OBP-301 treatment were evaluated by the fluorescent area of the liver tumor calculated by Cell software using GFP images obtained with the Olympus OV100. The experimental data are presented as

mean \pm SD. Comparison of the tumor area between the treatment and control groups was analyzed using a two-tailed Student's *t* test.

Viral GFP Labeling of Tumors

To assess the tumor detection ability of OBP-401 for metastatic liver tumors, a liver metastasis model of unlabeled HCT-116 cells was used. OBP-401 was injected i.v. or intrasplenically at a dose of 1×10^8 PFU/mouse. Animals were examined at laparotomy by fluorescence imaging with the OV100 5 days after OBP-401 was administered. Some mice

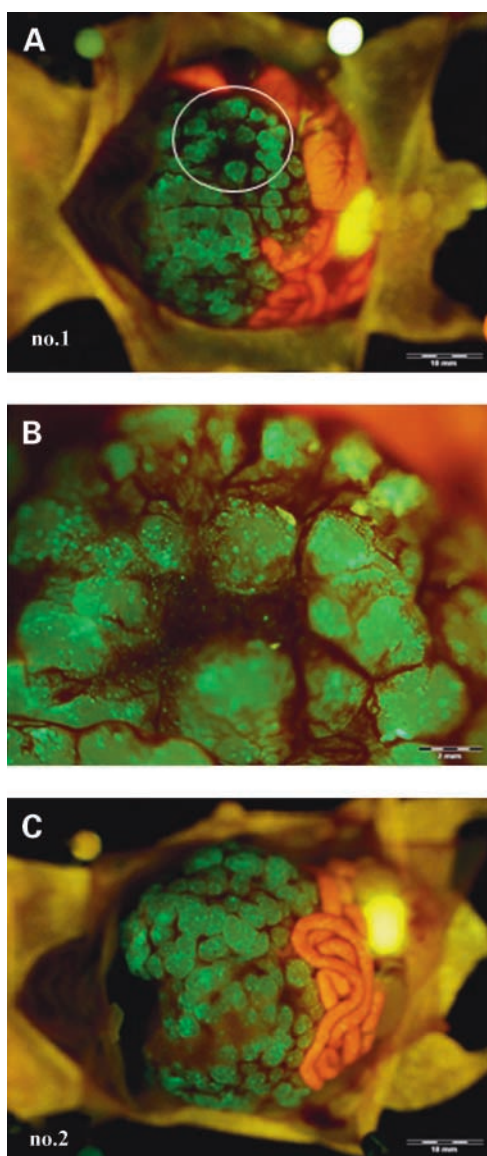


Figure 3. Portal venous delivery of OBP-401 selectively labeled multiple colon cancer liver metastases. **A**, gross appearance of the abdominal cavity (mouse no. 1). Five days after splenic injection of OBP-401, HCT-116 liver metastases were visualized by GFP fluorescence. **B**, higher magnification of the liver surface indicated by the white circle in **A**. **C**, liver metastases were visualized by GFP fluorescence in mouse no. 2.

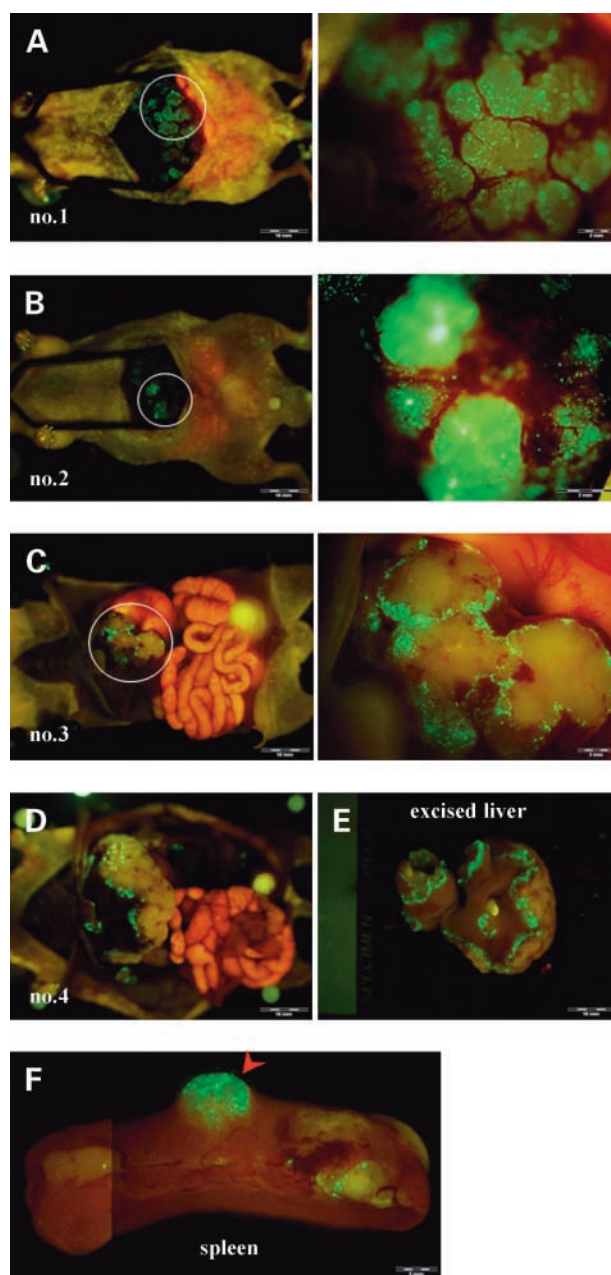


Figure 4. Selective GFP labeling of multiple liver metastases of human colon cancer by i.v. injection of OBP-401. **A** to **C**, 5 d after i.v. injection with OBP-401, HCT-116 liver metastases were visualized by GFP fluorescence (mouse nos. 1-3; *left*). Higher magnification of the liver metastasis indicated by a white circle (*right*). **D**, gross appearance of the abdominal cavity (mouse no. 4). **E**, macroscopic appearance of excised liver in mouse no. 4. The margin of the liver metastasis was visualized by GFP fluorescence. **F**, macroscopic appearance of spleen. Tumor development in the spleen was also visualized by GFP fluorescence 5 d after OBP-401 treatment (*red arrow*).

had a second-look observation 1 week after the first open examination.

To assess the tumor detection ability of OBP-401 in the orthotopic liver tumor model, unlabeled Hep3B cells were

used. OBP-401 was injected systemically into the tail vein at a dose of 1×10^8 PFU/mouse 2 weeks after tumor cell inoculation. Animals were examined at laparotomy by fluorescence imaging with the OV100 5 days after OBP-401 was administered. Some mice had a second-look observation 4 weeks after i.v. injection of OBP-401.

Fluorescence Optical Imaging and Processing

The Olympus OV100 Imaging System containing an MT-20 light source was used. High-resolution images are captured directly on a PC (Fujitsu Siemens), and images are analyzed with the use of Cell software (Olympus-Biosystems).

Results and Discussion

Liver Metastasis Model of Human Colon Cancer

Intrasplenic inoculation of nude mice with unlabeled HCT-116 or HCT-116-GFP human colon cancer cells led to multiple experimental metastases in the liver within 14 days. With HCT-116-GFP, spleen tumors and lung metastasis could also be observed by fluorescence imaging at 6 weeks after cancer cell implantation.

Orthotopic Liver Tumor Model of HCC

When unlabeled Hep3B or Hep3B-GFP human HCC cells were subserosally injected into the liver of nude mice (Fig. 1A), a small tumor mass (~2 mm) was often observed on the liver surface by 2 weeks after cancer cell inoculation. Hep3B liver tumors usually grew only in the injected lobe and rarely spread to other lobes (Fig. 1B). These tumors showed abundant tumor blood vessels, indicating a rich

blood supply for the tumor, which reflects HCC in human patients (Fig. 1C).

Unlabeled HepG2 cells were also inoculated in the spleen of nude mice with the same technique used in the experimental colorectal liver metastasis model. Two weeks after tumor cell inoculation, multiple HepG2 tumors were observed on the liver surface.

Inhibition of Experimental Colon Cancer Metastasis by OBP-301

OBP-301 was i.v. injected at a dose of 5×10^8 PFU/mouse 5 days after HCT-116-GFP inoculation in the spleen. At 6 weeks after HCT-116-GFP colon cancer cell inoculation, 100% of the control animals developed liver tumors, and tumors in the spleen developed in 40% of control animals. Treatment with OBP-301 caused a significant inhibition in liver metastasis growth ($P < 0.05$; Fig. 2A and D). Additionally, OBP-301-treated animals showed a reduced number of lung metastases colonies compared with controls ($P < 0.05$; Fig. 2B and E). These results show that systemic dosing of OBP-301 has significant antitumor activity against experimental colon cancer liver metastasis. In contrast to the experimental liver metastasis, OBP-301 did not have an apparent effect on the spleen tumors. The lack of effect of OBP-301 on the spleen tumors may be because of their very small size, which made differences difficult to discern.

Inhibition of Orthotopic HCC by OBP-301

To evaluate the antitumor efficacy of OBP-301 on HCC tumors, the orthotopic liver tumor model of Hep3B-GFP was used.

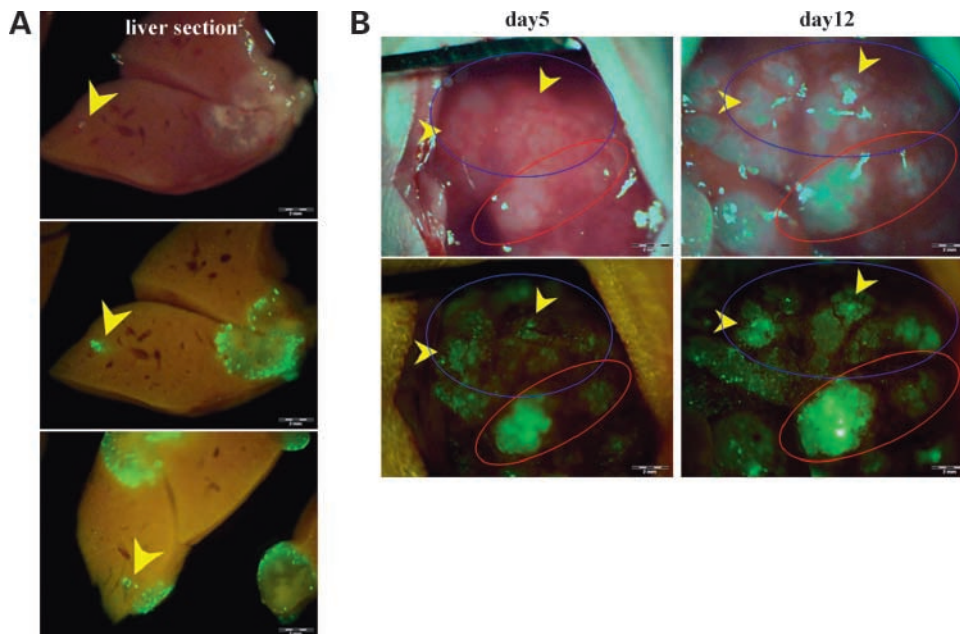


Figure 5. Early metastatic liver tumors not otherwise clearly visible could be visualized after i.v. injection of OBP-401. **A**, cross-sections of liver. GFP expression was mainly located at the periphery of the liver metastases. Tiny metastatic foci not otherwise clearly visible were visualized by GFP fluorescence after i.v. injection of OBP-401 (yellow arrow). **B**, 5 d after i.v. injection of OBP-401, HCT-116 liver metastases were visualized by GFP fluorescence (red circle). There were areas in the liver, which had GFP expression but seemed to be tumor-free in bright light (blue circle). Seven days later, metastases could be visualized by bright light as well as GFP fluorescence (yellow arrows), showing the power of OBP-401 to label very early, otherwise invisible metastases with GFP.

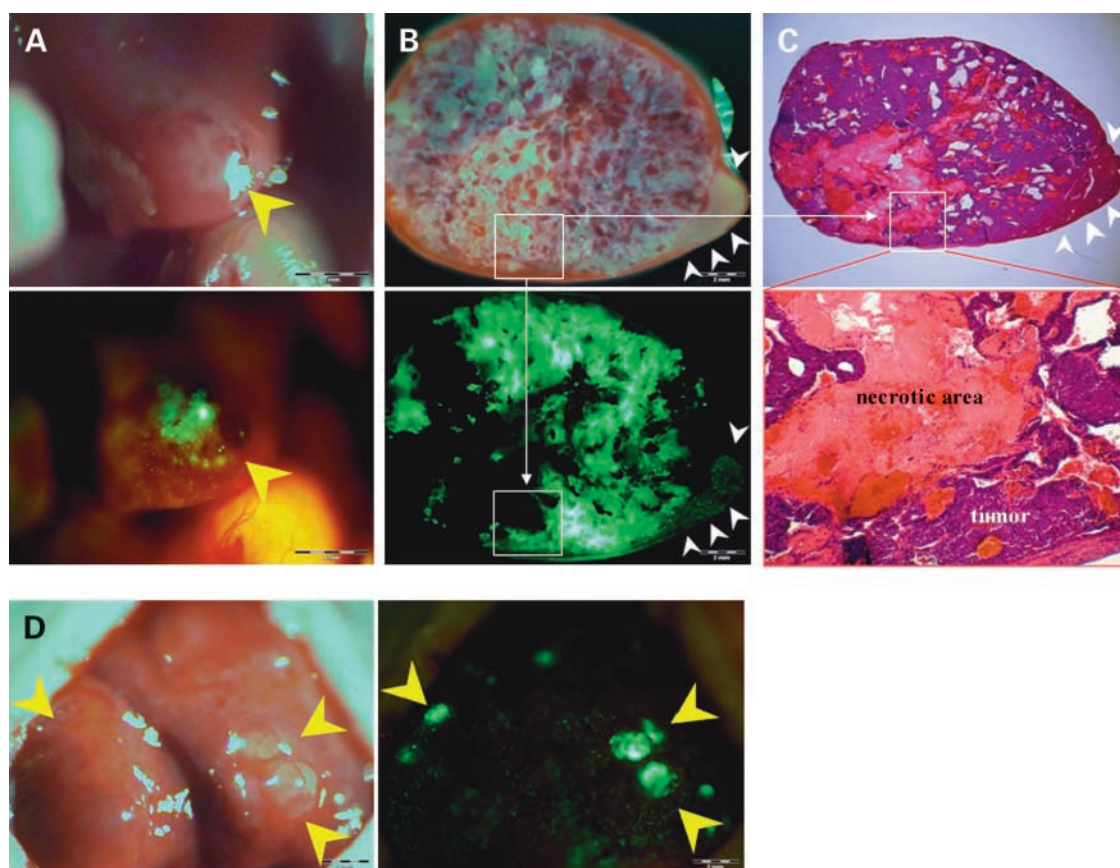


Figure 6. Selective visualization of orthotopic HCC tumors by i.v. injection of OBP-401. **A**, 5 d after systemic administration of OBP-401, orthotopic Hep3B HCC was visualized by GFP fluorescence (yellow arrow). *Top*, bright-field observation; *bottom*, fluorescence detection. **B**, cross-section of liver tumor 4 wk after i.v. injection of OBP-401. GFP expression was selectively detected in the tumor. White arrow indicates normal liver tissue. *Top*, bright-field observation; *bottom*, fluorescence detection. **C**, H&E section of Hep3B liver tumor of **B**. *Top*, magnification, $\times 10$; *bottom*, detail of the boxed region. Magnification, $\times 40$. Boxes refer to corresponding regions in **B** and **C** with high magnification in **B** and **C** (*bottom*). **D**, orthotopic HepG2 HCC tumors (yellow arrows) were visualized by GFP fluorescence (yellow arrows) 4 wk after i.v. injection of OBP-401.

The colorectal liver metastasis model was made by delivering cells into the portal vein as described above, whereas the orthotopic HCC model was made by injecting cells directly into the hepatic parenchyma, where at the early stage of tumor development most cells were thought to locate outside of the blood vessels. Thus, i.v. injected OBP-301 could target cancer cells more effectively in the colorectal liver metastasis model than in the HCC model. In the HCC model, therefore, we increased the number of injections of OBP-301, which was administered biweekly (5×10^8 PFU/2 weeks i.v. for 6 weeks) starting 2 weeks after tumor cell inoculation. Treatment of OBP-301 caused a significant inhibition in liver tumor growth ($P < 0.01$; Fig. 1D and E). These results show that systemic dosing of OBP-301 has significant antitumor activity against Hep3B-GFP human HCC tumors.

Selective Visualization of Colorectal Liver Metastases by OBP-401 Delivery of the GFP Gene

To assess the tumor detection ability of OBP-401 for colorectal liver metastases, OBP-401 was administrated to mice by portal venous delivery or systemic delivery using the tail vein.

Animals with HCT-116 experimental liver metastases were intrasplenically injected with OBP-401 (1×10^8 PFU/mouse) 12 days after tumor cell inoculation. The spleen was used to access the portal venous circulation. Five days after injection of OBP-401, the liver metastases could be visualized by GFP fluorescence. Representative mice are shown in Fig. 3. Cross-sections of the liver showed that GFP fluorescence occurred mainly at the periphery of the metastatic liver nodules (data not shown). Liver metastases in mice given 1×10^7 PFU of OBP-401 were not visualized efficiently by GFP expression (data not shown), indicating dose response.

HCT-116 liver metastases could also be visualized by GFP fluorescence after i.v. injection of OBP-401 (1×10^8 PFU/mouse; Fig. 4). Cross-sections of the liver also showed tiny metastatic foci visualized by GFP fluorescence (Fig. 5A). Moreover, a second-look observation done 1 week after the first laparotomy showed that early metastatic liver tumors, not clearly visible under bright light, had been visualized with GFP fluorescence after i.v. injection of OBP-401 at as early as day 5, indicating the possibility of early

detection of metastatic disease (Fig. 5B). When injected with more than 2×10^8 PFU of OBP-401, mice often showed GFP fluorescence in normal tissues such as liver, lung, spleen, and thoracic duct (data not shown). These results suggest that colorectal liver metastases can be visualized by GFP fluorescence both by portal venous and i.v. administration of OBP-401.

Selective Visualization of Orthotopic HCC by OBP-401

Five days after injection of OBP-401 (1×10^8 PFU/mouse) into the tail vein, HCC liver tumors were visualized by GFP fluorescence (Fig. 6A). Cross-sections of the liver at 4 weeks after i.v. injection of OBP-401 showed that GFP expression was in the cancer cells and not in normal cells (Fig. 6B and C). Small liver tumor nodules were also visualized by GFP fluorescence after i.v. OBP-401 administration (Fig. 6D). Thus, we showed that HCC liver tumors could be selectively visualized by GFP fluorescence after i.v. injection of OBP-401.

Many studies have shown that the majority of malignant human tumors tested express hTERT. OBP-301 and OBP-401 specifically replicate in tumors due to hTERT expression in tumors (11, 12, 17–19). In previous studies, OBP-301 and OBP-401 were administered locally, such as by intratumoral or intrapleural administration. The present report shows the systemic efficacy of OBP-301 and OBP-401 to selectively replicate in and kill and label primary and metastatic liver tumors after i.v. administration. Closely related virus constructs will be compared with OBP-301 and OBP-401 in the future.

Our laboratory pioneered the use of fluorescent proteins to visualize cancer cells *in vivo*. Cancer cells genetically labeled by fluorescent proteins have increased the possibility and sensitivity to observe progression of cancer cells in live animals (21). To evaluate antitumor efficacy of i.v. administration of OBP-301 against primary and metastatic liver tumors, we used GFP-expressing human cancer cell lines. We showed that i.v. administration of OBP-301 resulted in a significant reduction in experimental liver and pulmonary metastases in a colorectal liver metastases model and effectively inhibited tumor formation and growth in an orthotopic HCC model. OBP-401 has less but still significant cytotoxic effects compared with OBP-301 (22). In fact, a significant inhibition of tumor growth by intratumoral injection of OBP-401 was confirmed *in vivo* in our previous study (20). However, OBP-401 at the tumor-selective labeling dose used in this i.v. injection study could not inhibit tumor growth effectively.

The imaging strategy using OBP-401 has a potential of being available in humans as a navigation system in the surgical treatment of malignancy. During surgery, tumors that would be difficult to detect by direct visual detection could be positively identified with GFP fluorescence using a handheld excitation light and appropriate filter goggles as we have shown previously in mice (23–25). Employment of a fluorescence surgical microscope would enable visualization of the GFP-expressing microscopic leading edge of the tumor and allow accurate resection with sufficient margins.

As for toxicity of OBP-301 and OBP-401, only when injected with 5×10^8 PFU OBP-301 for the first time, a few mice showed lethargy but fully recovered within 1 h. None of the mice treated with OBP-301 or OBP-401 at the doses used in this study showed significant adverse effects during the observation period or histopathologic changes in the liver at the time of sacrifice. In the near future, the safety of OBP-301 will be confirmed in a phase I clinical trial, which is currently under way (26).

Our studies suggest the clinical potential of OBP-301 and OBP-401.

Disclosure of Potential Conflicts of Interest

No potential conflicts of interest were disclosed.

References

- Bruix J, Hessheimer AJ, Forner A, Boix L, Vilana R, Llovet JM. New aspects of diagnosis and therapy of hepatocellular carcinoma. *Oncogene* 2006;25:3848–56.
- Okuda K. Hepatocellular carcinoma. *J Hepatol* 2000;32:225–37.
- Takayasu K, Muramatsu Y, Moriyama N, et al. Clinical and radiologic assessments of the results of hepatectomy for small hepatocellular carcinoma and therapeutic arterial embolization for postoperative recurrence. *Cancer* 1989;64:1848–52.
- Koshariya M, Jagad RB, Kawamoto J, et al. An update and our experience with metastatic liver disease. *Hepato-gastroenterology* 2007;54:2232–9.
- Kavolius J, Fong Y, Blumgart LH. Surgical resection of metastatic liver tumors. *Surg Oncol Clin N Am* 1996;5:337–52.
- Chouillard E, Cherqui D, Tayar C, Brunetti F, Fagniez PL. Anatomical bi- and trisegmentectomies as alternatives to extensive liver resections. *Ann Surg* 2003;238:29–34.
- Jiao LR, Hansen PD, Havlik R, Mitry RR, Pignatelli M, Habib N. Clinical short-term results of radiofrequency ablation in primary and secondary liver tumors. *Am J Surg* 1999;177:303–6.
- Khatrri VP, Petrelli NJ, Belghiti J. Extending the frontiers of surgical therapy for hepatic colorectal metastases: is there a limit? *J Clin Oncol* 2005;23:8490–9.
- Adam R. Chemotherapy and surgery: new perspectives on the treatment of unresectable liver metastases. *Ann Oncol* 2003;14 Suppl 2:ii13–6.
- Bismuth H, Adam R, Lévi F, et al. Resection of nonresectable liver metastases from colorectal cancer after neoadjuvant chemotherapy. *Ann Surg* 1996;224:509–20, discussion 520–2.
- Kawashima T, Kagawa S, Kobayashi N, et al. Telomerase-specific replication-selective virotherapy for human cancer. *Clin Cancer Res* 2004;10:285–92.
- Taki M, Kagawa S, Nishizaki M, et al. Enhanced oncolysis by a tropism-modified telomerase-specific replication-selective adenoviral agent OBP-405 ('telomelysin-RGD'). *Oncogene* 2005;24:3130–40.
- Umeoka T, Kawashima T, Kagawa S, et al. Visualization of intrathoracically disseminated solid tumors in mice with optical imaging by telomerase-specific amplification of a transferred green fluorescent protein gene. *Cancer Res* 2004;64:6259–65.
- Hashimoto Y, Watanabe Y, Shirakiya Y, et al. Establishment of biological and pharmacokinetic assays of telomerase-specific replication-selective adenovirus. *Cancer Sci* 2008;99:385–90.
- Kishimoto H, Kojima T, Watanabe Y, et al. *In vivo* imaging of lymph node metastasis with telomerase-specific replication-selective adenovirus. *Nat Med* 2006;12:1213–9.
- Takakura M, Kyo S, Kanaya T, et al. Cloning of human telomerase catalytic subunit (hTERT) gene promoter and identification of proximal core promoter sequences essential for transcriptional activation in immortalized and cancer cells. *Cancer Res* 1999;59:551–7.
- Watanabe T, Hioki M, Fujiwara T, et al. Histone deacetylase inhibitor FR901228 enhances the antitumor effect of telomerase-specific

- replication-selective adenoviral agent OBP-301 in human lung cancer cells. *Exp Cell Res* 2006;312:256–65.
18. Hioki M, Kagawa S, Fujiwara T, et al. Combination of oncolytic adenovirotherapy and Bax gene therapy in human cancer xenografted models. Potential merits and hurdles for combination therapy. *Int J Cancer* 2008;122:2628–33.
19. Huang P, Watanabe M, Kaku H, et al. Direct and distant antitumor effects of a telomerase-selective oncolytic adenoviral agent, OBP-301, in a mouse prostate cancer model. *Cancer Gene Ther* 2008;15:315–22.
20. Fujiwara T, Kagawa S, Kishimoto H, et al. Enhanced antitumor efficacy of telomerase-selective oncolytic adenoviral agent OBP-401 with docetaxel: preclinical evaluation of chemovirotherapy. *Int J Cancer* 2006;119:432–40.
21. Hoffman RM. The multiple uses of fluorescent proteins to visualize cancer *in vivo*. *Nat Rev Cancer* 2005;5:796–806.
22. Kyo S, Takakura M, Fujiwara T, Inoue M. Understanding and exploiting hTERT promoter regulation for diagnosis and treatment of human cancers. *Cancer Sci* 2008;99:1528–38.
23. Yang M, Luiken G, Baranov E, Hoffman RM. Facile whole-body imaging of internal fluorescent tumors in mice with an LED flashlight. *Biotechniques* 2005;39:170–2.
24. Kishimoto H, Zhao M, Hayashi K, et al. *In vivo* internal tumor illumination by telomerase-dependent adenoviral GFP for precise surgical navigation. *Proc Natl Acad Sci U S A* 2009;106:14514–7.
25. Jasni BR. Green surgery. *Science* 2009;325:1321.
26. Fujiwara T, Tanaka N, Numunaitis JJ, et al. Phase I trial of intratumoral administration of OBP-301, a novel telomerase-specific oncolytic virus, in patients with advanced solid cancer. Evaluation of biodistribution and immune response. *J Clin Oncol* 2008;26:3572.